Chemical Science

Cite this: *Chem. Sci.*, 2011, **2**, 1121

www.rsc.org/chemicalscience

EDGE ARTICLE

A hybrid magnet with coexistence of ferromagnetism and photoinduced Fe(III) spin-crossover†

Miguel Clemente-León,*[a] Eugenio Coronado,*[a] Maurici López-Jordà,[a] Cédric Desplanches,[b] Saket Asthana,[b] Hongfeng Wang[b] and Jean-François Létard[b]

Received 11th January 2011, Accepted 4th March 2011
DOI: 10.1039/c1sc00015b

The insertion of a $[Fe(sal_2\text{-trien})]^+$ complex cation into a 2D oxalate network results in a hybrid magnet with coexistence of magnetic ordering and photoinduced spin-crossover (LIESST effect) in compound $[Fe^{III}(sal_2\text{-trien})][Mn^{II}Cr^{III}(ox)_3]\cdot(CH_2Cl_2)$ (**1**). A complete photomagnetic characterization together with a detailed structural analysis of the low-spin (LS) and high-spin (HS) structures of **1** is presented in order to understand such unusual behavior. This very rare and unexpected property in a Fe^{III} spin-crossover complex, has been attributed to the strong distortion exhibited by the metastable HS state. Furthermore, **1** has shown that, in contrast to what has been previously proposed, a cooperative spin-crossover is not a necessary condition to observe LIESST effect in Fe^{III} compounds. The photo-induced spin conversion of the inserted Fe^{III} complex has shown to have a negligible influence on the cooperative magnetic behaviour of the 2D oxalate network.

Introduction

Multifunctionality is one of the most appealing topics in chemical science. A rational approach to design multifunctional materials consists of building up two-network hybrid solids formed by two molecular fragments where each network furnishes distinct physical properties. If the two networks are quasi-independent, a coexistence of the two physical properties is anticipated.[1] If the two molecular networks are coupled, an interplay between their properties may be observed.[1b] Finally, if one of these two networks is physically (or chemically) responsive (*i.e.*, if it changes its properties under the application of an external stimulus, like for example light, pressure or temperature), a switchable multifunctional material can be obtained in which the responsive network can influence the properties of the other network.[2]

Bimetallic oxalate-bridged complexes of formula $A[M^{II}M^{III}(ox)_3]$ (M^{III} = Cr, Fe, Ru, V, Mn; M^{II} = Mn, Fe, Co, Ni, Cu, Zn; A = Cation; ox = oxalate) have provided remarkable examples of these types of materials.[3] They are composed by polymeric 2D[4] or 3D[5] anionic networks, which furnish the cooperative magnetic properties (ferro-, ferri- or canted antiferromagnetism), and a bulky charge-compensating molecular cation, which templates the network formation and adds a second physical property to the solid. The insertion of different cations into oxalate networks has led to compounds combining the long-range magnetic ordering from the oxalate network with paramagnetism,[6] photochromism,[7] electric conductivity,[8] proton conduction,[9] chirality[10] or very recently, chirality and conductivity in the same compound.[11]

The interplay between the properties of the two molecular networks has been observed, for example, in enantiopure 2D oxalate-based magnets prepared by Train *et al.* that exhibit magneto-chiral dichroic effect and magnetisation-induced second harmonic generation.[12]

The design of switchable magnets has been less explored. A promising approach to reach this goal consists of combining the bimetallic oxalate network with spin-crossover complexes. These kinds of molecular complexes change their spin state from low-spin (LS) to high-spin (HS) configurations when submitted to an external stimulus such as temperature, light-irradiation or pressure. As this magnetic switching is accompanied by changes in the molecular size, the spin-crossover process should act as an internal pressure in the hybrid material and therefore, it might affect the long-range magnetic ordering in the extended magnetic network.

Although several compounds combining spin-crossover cations and bimetallic oxalate anion networks have been reported,[13,14] the only one showing coexistence of spin-crossover and ferromagnetism is $[Fe^{III}(sal_2\text{-trien})][Mn^{II}Cr^{III}(ox)_3]\cdot(CH_2Cl_2)$ (**1**) reported very recently by our group.[14] This compound is formed by $[Fe(sal_2\text{-trien})]^+$ cations inserted between $Mn^{II}Cr^{III}$ bimetallic

[a]*Instituto de Ciencia Molecular, Universidad de Valencia, Catedrático José Beltrán 2, Paterna, 46980, Spain. E-mail: miguel.clemente@uv.es; Fax: +34 963543273; Tel: +34 963544405; eugenio.coronado@uv.es*
[b]*CNRS, Université de Bordeaux, ICMCB, 87 avenue du Dr A. Schweitzer, Pessac, F-33608, France*

† Electronic supplementary information (ESI) available: crystallographic data, intermolecular interactions, ZFC and FC magnetisation and AC measurements before and after irradiation, and details of the fitting of the magnetism of $[Mn^{II}Cr^{III}(ox)_3]$ layers. CCDC reference numbers 807172, 807173, 813345, 813714. For ESI and crystallographic data in CIF or other electronic format see DOI: 10.1039/c1sc00015b

oxalate layers. It presents a gradual spin-crossover transition from 350 to 160 K, and a ferromagnetic ordering at 5.6 K. Furthermore, by changing the synthetic conditions a second compound of formula $[Fe^{III}(sal_2\text{-trien})][Mn^{II}Cr^{III}(ox)_3]\cdot(CH_3OH)$ (**2**) has also been obtained. This compound shows an unusual non-chiral 3D network with inserted $[Fe(sal_2\text{-trien})]^+$ cations, exhibiting a gradual spin-crossover of 30% of the Fe(III) from 300 to 130 K, together with a ferromagnetic ordering at 5.2 K. Unfortunately, in these compounds no interplay between these two properties—spin-crossover and ferromagnetism—has been detected. This is probably due to the large difference in temperature at which the two phenomena occur. Thus, while the spin-crossover occurs at high temperatures (in the range 130–350 K), the ferromagnetic ordering occurs below 5.2–5.6 K.

A way to overcome this limitation is to take advantage of the photo-induced spin-crossover effect, also known as LIESST effect (light-induced excited spin-state trapping).[15] This phenomenon was originally established for Fe^{II} complexes at low-temperatures (typically below 50 K).[16] In principle, the relaxation *via* a tunneling process from the HS to the LS state is much faster in Fe^{III} compounds because the changes in the metal–ligand bond lengths between the two states are significantly smaller. However, there are two examples of Fe^{III} complexes showing the LIESST effect reported by Sato *et al.*[17,18] The explanation given by these authors for such unexpected behavior is related to the large structural distortion between the LS and HS states, with the intermolecular interactions playing an important role in the relaxation behavior.[18]

In this work, we will explore the possibility of using light irradiation to induce spin-crossover in these hybrid materials. We will show that the confinement of $[Fe(sal_2\text{-trien})]^+$ cations provided by the 2D bimetallic oxalate layers in **1** can also induce LIESST effect in Fe^{III} complexes. A complete photomagnetic characterization together with a detailed structural analysis of the LS and HS structures of **1** is presented in order to understand such unusual behavior. Finally, the possibility of using this family of compounds as switching magnets will be explored.

Results

Crystal structure of 1

The syntheses, crystal structures, Mössbauer spectroscopy and magnetic properties of **1** and **2** were reported previously.[14] In this work, four crystal structures of **1** at 92, 120, 250 and 300 K were solved to study the structural changes between the LS and HS structures.[19] Furthermore, we used for comparison the structural data at 180 K from the previous work[14] and measured the unit cell of one crystal between 92 and 290 K.

The structure of **1** is formed by anionic $[MnCr(ox)_3]^-$ sheets in the *bc* plane alternating with inter-lamellar $[Fe(sal_2\text{-trien})]^+$ cations and dichloromethane solvent molecules (see Fig. 1 and Fig. 2).

To evaluate the structural distortion between the LS and HS octahedral coordination geometries of $[Fe(sal_2\text{-trien})]^+$ in **1**, we have focused on the differences observed in the crystal structures measured at 120 and 300 K for the same crystal because they correspond roughly to the LS and HS structures.

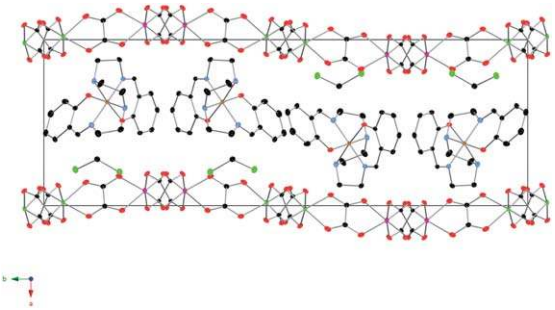

Fig. 1 Projection of the structure of **1** in the *ab* plane at 120 K. Fe (yellow), Cl (green) C (black), N (blue), O (red) Mn(pink), Cr(green). Hydrogen atoms have been omitted for clarity.

The first difference is a shortening of metal–ligand bond lengths as expected for a spin-crossover. Thus, the average Fe–N and Fe–O bond distances in the structure solved at 300 K are respectively, 2.124(4) and 1.890(4) Å, while those solved at 120 K are 1.975(2) and 1.866(2) Å. This results in average bond length differences $\Delta r_{HL,Fe-N} = 0.149$ Å and $\Delta r_{HL,Fe-O} = 0.024$ Å.

The second difference concerns the distortion of the octahedral coordination site, which is significantly larger for the HS state. Thus, at 300 K two of the three diagonals from the octahedron, defined by the bonds N(amine)–Fe–O(phenoxo) (N(amine) = N2,N3), differ strongly from 180° (158.08(19) and 161.23(15)°), while the remaining one, defined by the bond N(imine)–Fe–N(imine), is 176.78(15)° (N(imine) = N1,N4). On the contrary, the coordination octahedron is much more regular at 120 K. The three diagonals are much closer to 180° with N(amine)–Fe–O(phenoxo) angles of 173.18(10) and 173.82(9)° and N(imine)–Fe–N(imine) angle of 179.63(11)°. Different parameters have been used by several authors to quantify the distortions of $[Fe(sal_2\text{-trien})]^+$ salts, such as Σ and Θ (see Table 1).[20–22] As expected, angular and trigonal distortions, which are evaluated respectively by Σ and Θ, are much more important when the Fe^{III} complex is in the HS state (300 K). On the other hand, Σ and Θ parameters of the LS structures (92, 120 and 180 K) present very similar values while the structure with intermediate spin state (250 K) present intermediate values between the LS and HS structures as expected (see Table 1).

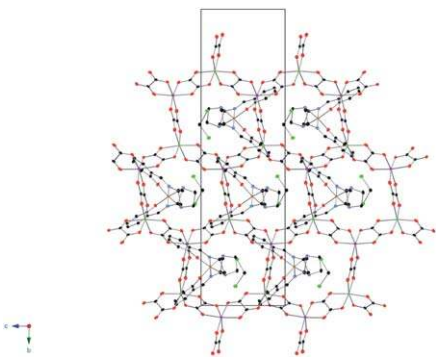

Fig. 2 Projection of the structure of **1** in the *bc* plane at 120 K. Fe (yellow), Cl (green) C (black), N (blue), O (red) Mn(pink), Cr(green). Hydrogen atoms have been omitted for clarity.

Table 1 Structural parameters of **1** and **2**

	Spin state	Mean Fe–N (Å)	Mean Fe–O (Å)	Σ (°)[a]	Θ (°)[b]
1 (300 K)	~ 80% HS	2.124(4)	1.890(4)	88	244
1 (250 K)	~ 50% HS	2.076(4)	1.871(3)	72	217
1 (180 K)	~ 90% LS	1.989(4)	1.866(3)	52	89
1 (120 K)	LS	1.975(2)	1.866(2)	49	87
1 (92 K)	LS	1.978(3)	1.864(2)	50	86
2 (120 K) [Fe1]	~ 72% HS	2.039(15)	1.886(12)	71	190
[Fe2]		2.14(2)	1.859(14)	89	235

[a] $\Sigma = \sum_{i=1}^{12} |90 - \alpha_i|$ where α_i are the 12 *cis*-N/O–Fe–N/O angles around the iron atom. [b] $\Theta = \sum_{j=1}^{24} |60 - \theta_j$ where θ_j are the 24 unique N/O–Fe–N/O angles measured on the projection of two triangular faces of the octahedron along their common pseudo-threefold axis.

The third difference concerns the structural disorder shown by one of the ethylene groups at 300 K, which can be solved by considering two possible configurations with occupancies of 58 and 42%. This disorder is not observed in the structures close to the LS state at 180, 120 and 92 K but it is maintained in the structure with ~50% of Fe^{III} in the HS state (250 K) with occupancies of 56 and 44%. Dichloromethane molecules that occupy the holes left by the $[Fe(sal_2\text{-trien})]^+$ cations and the oxalate network, present a similar disorder at 250 and 300 K, which disappears at 92, 120 and 180 K.

The crystal packing of $[Fe(sal_2\text{-trien})]^+$ complexes between the low and high temperature structures also presents some changes, which are reflected in the lattice parameters. Changes in the unit cell of **1** indicate a shortening of *a* and *b* axis from 300 to 92 K whereas the *c* axis remains almost constant with a small increase at decreasing temperature (see Fig. S1†). Furthermore, the β angle decreases gradually from 300 to 92 K. All these changes are more important in the spin-crossover region from 300 to 175 K indicating that they are associated with the change of spin state of $[Fe(sal_2\text{-trien})]^+$. To understand these changes, let us first describe the intermolecular contacts between the Fe^{III} complexes. In the present case, this packing is restricted in the *bc* plane as the Fe^{III} complexes are confined between two anionic bimetallic oxalate layers. They lie with their longer axis parallel to the oxalate layers, and they are connected through edge-to-face C–H···π and N–H···π interactions[23] (see Figs. S2 and S3†) forming double chains running along the *c* axis. From the two phenoxy rings of sal_2-trien, only the one placed in the internal part of the double chain is involved in these C–H···π and N–H···π interactions with four adjacent Fe^{III} complexes belonging to the same double chain. Furthermore, the phenoxy ring belonging to different double chains present π–π stacking interactions. Finally, there are numerous short contacts with the oxalate ligands of the two neighboring layers (see Figs S4 and S5†).

As the *a* parameter gives the separation between the oxalate layers (from 12.096(5) Å at 300 K to 11.5561(3) Å at 120 K), the shortening of *a* axis arises from the change in the spin state of the Fe^{III} complex. The most important consequence of this shortening is that at 120 K there are shorter contacts between O atoms from oxalate layers and CH groups from $[Fe(sal_2\text{-trien})]^+$ (see SI†). On the other hand, the most important effect of the shortening of *b* axis (from 32.135(5) Å at 300 K to 31.6369(7) Å at 120 K) is the presence of shorter contacts at 120 K between Fe^{III} complexes belonging to the same double chains through N–H···π edge-to-face interactions and between Fe^{III} complexes belonging to different double chains through π–π stacking interactions. On the contrary, offset π–π stacking interactions appear in the structure at 300 K between C atoms of phenoxy rings belonging to different double chains (in green in Figure S2†) with weaker contacts in the structure solved at 120 K (see SI†).

Change in the magnetic properties of 1 upon irradiation

In Fig. 3, we plot the magnetic behavior of **1** before and after light irradiation. Before irradiation χT shows a constant value of 10.0 emu·K mol^{-1} in the high temperature range (from 400 to 350 K), which is approximately equal to the sum of the expected contributions for the isolated paramagnetic ions with ~80% of Fe^{III} spin-crossover complex in a HS state. From 350 to 165 K, χT decreases gradually to reach a minimum χT value at 165 K of 7.2 emu·K mol^{-1}. This value is consistent with the Mössbauer data that indicates that Fe^{III} is 94% LS at this temperature.[14] Therefore, in this range of temperatures a HS → LS spin conversion of the Fe^{III} complex takes place. Below 165 K, χT increases due to the Mn^{II}–Cr^{III} ferromagnetic interactions within the bimetallic oxalate layers. This increase is very sharp at lower temperatures suggesting the onset of long-range ferromagnetic ordering at 5.6 K, as confirmed by AC susceptibility and field cooled (FC) and zero-field cooled (ZFC) magnetization measurements (Figs. S6 and S7†).[14]

During irradiation at 647 nm wavelength (power 8 mW cm^{-2}), at 10 K inside a SQUID cavity, an increase in χT was observed at low temperatures. Thus, after about 1.5 h the light irradiation was switched off. The temperature was then increased at 0.3 K min^{-1} and the magnetic susceptibility recorded. Below 50 K, the χT value after irradiation is clearly higher than the one before irradiation, while above 50 K, the two curves are superimposed (Fig. 3). This result suggests that a photomagnetic effect has occurred, which can be attributed to the spin photoconversion of

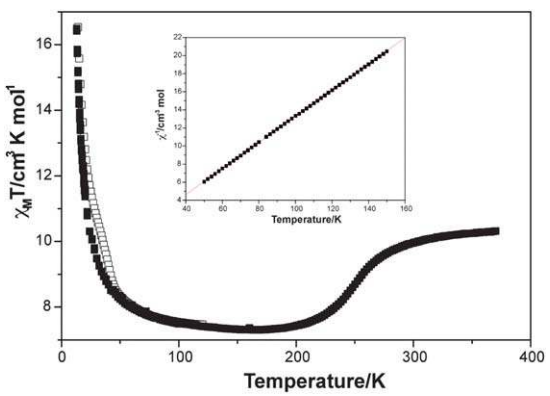

Fig. 3 Magnetic and Photo-Magnetic behaviour for compound **1**. ■ Magnetic behaviour measured in dark. □ Photo-magnetic behaviour measured after irradiation by 647 nm wavelength laser. Inserted graph: Curie–Weiss law between 50 K and 150 K.

the [Fe(sal$_2$-trien)]$^+$ from its LS ground state at low temperature to its HS metastable state. In order to estimate the fraction of photoconverted Fe^{III}, the magnetism of the Mn^{II}Cr^{III} bimetallic layers needs to be substrated as it presents a strong underlying magnetism. To estimate the magnetism of the bimetallic layers we have taken advantage of the fact that below the thermal spin transition (*i.e.* below 150 K) and well above the Curie temperature (*i.e.* above 50 K), the magnetic response can be satisfactorily simulated by a Curie–Weiss law (see inset in Fig. 3). Below 50 K, this simple Curie–Weiss law is unable to reproduce properly the χT values due to the vicinity of the ferromagnetic ordering. In this region, we have used the molecular field model proposed by Néel that explicitly takes into account the fact that there are two distinct sub-networks in the Mn^{II}Cr^{III} layers.[24] Differences between experimental χT values and those obtained with this model are lower than 0.04 cm^3 K mol^{-1} in between 25 K and 175 K. Details of this fitting are given as supporting information.† In Fig. 4, we plot the temperature dependence of the fraction of HS Fe^{III} (γ_{HS}) before and after irradiation after subtracting the contribution from the Mn^{II}Cr^{III} oxalate network.

γ_{HS} is almost zero below 170 K in the measurements performed in the dark. Increasing the temperature above 170 K leads to a gradual increase of γ_{HS} with a maximum value of 0.86 at 370 K in agreement with Mössbauer measurements.[14] γ_{HS} from the curve obtained after irradiation reaches a maximum value of 0.37 at 25 K. When the temperature increases, a decrease in γ_{HS} is observed, and γ_{HS} reaches 0 at about 75 K. At higher temperatures γ_{HS} curve is superimposed with that recorded in the dark. The T(LIESST), estimated from the minimum of the derivative of γ_{HS} by the temperature (inset in Fig. 4), is determined to be 41 K.[25] This represents somewhat the limit of the long-lived photo-induced lifetime of the HS state. In order to get some insight into the decay of the photoinduced HS state, some kinetics have been recorded at 10 K and every 2 K between 36 and 44 K (Fig. 5).

At 10 K, almost no decay of the photo-induced HS state was noticed. More precisely, the decrease of the HS fraction was less than 2% after 7 h. Fig. 5 shows the relaxation kinetics recorded between 36 and 44 K. The maximum of HS fraction at initial time, for a given kinetic is different: the higher the temperature, the lower the photoexcitation. This suggests that the kinetic process is thermally activated. Interestingly, these relaxation curves show strong deviation from a single exponential, with a marked stretched exponential behaviour, and with a fast component at earlier times and a long decay process at infinite time. For reproducing this type of curves, Hauser *et al.*[26] used a distribution of relaxation rates at a given temperature with a Gaussian distribution of the activation energy. Following this procedure, the relaxation curves of compound **1** can be satisfactorily fitted as illustrated by the solid lines in Fig. 5. The apparent activation energy, E_a (= 200 cm^{-1}), and the apparent preexponential factor, k_∞ (= 0.49 s^{-1}) of the activated region are calculated from the straight line of the $\ln k_{HL}(T)$ *vs.* $1/T$ plot. The standard deviation of the activation energy is 52 ± 6 cm^{-1}.

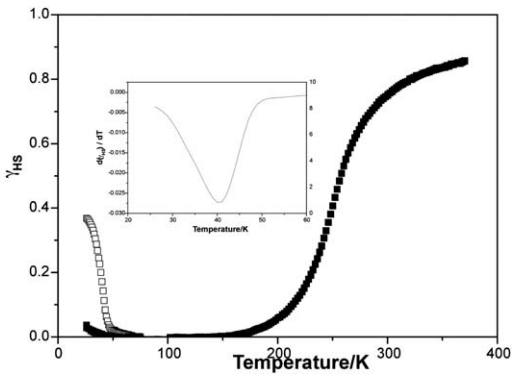

Fig. 4 Fraction of HS Fe^{III} (γ_{HS}) before (■) and after (□) irradiation). Inserted graph: χT derivative for photo-magnetism.

Effect of photoexcitation on the magnetic ordering

FC and ZFC magnetization (Fig. S6†) and AC susceptibility measurements (Fig. S7†) have been recorded between 2 and 10 K, before and after photoirradiation of 1.5 h at 10 K to test if the photoconversion of the Fe^{III} complex affects the Curie temperature (T_c) of the compound. We have to take into account that at 10 K the lifetime of the photoinduced HS state is very long, and consequently the HS fraction remains almost constant during the experiment. ZFC and FC magnetization measurements start to bifurcate at 5.6 K, both before and after irradiation. Similarly, AC susceptibility measurements show the appearance of an out-of-phase signal (χ'') below T_c = 5.6 K that remains almost constant upon irradiation, showing a shift to higher values by 0.1 K after photoirradiation.

Crystal structure and photomagnetism of 2

The structure of **2** was solved at 120 K.[14] It is formed by an anionic 3D polymeric oxalate-bridged bimetallic network with [Fe(sal$_2$-trien)]$^+$ cations and methanol solvent molecules occupying the cavities. Magnetic measurements and Mössbauer spectroscopy[14] indicate that 100% of Fe^{III} complexes are in the HS at room temperature and the HS → LS spin conversion of 30% of the Fe^{III} complexes from 300 and 130 K. There are two crystallographically independent [Fe(sal$_2$-trien)]$^+$ complexes ([Fe1] and [Fe2]). The average Fe–N and Fe–O bond distances

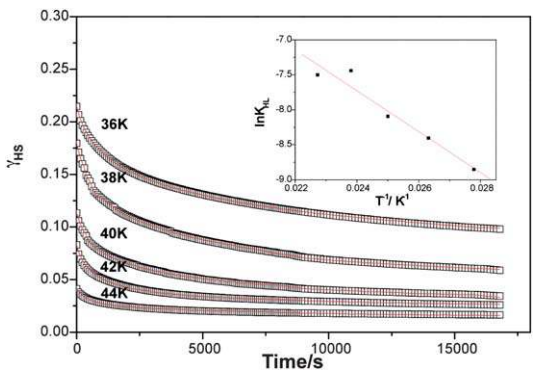

Fig. 5 Relaxation kinetics and simulation of the HS fraction *vs.* time at different temperatures. Inserted graph: $\ln k_{HL}(T)$ *vs.* $1/T$ dependence. k_{HL}corresponds to the rate constant for the HS → LS relaxation. The fitting procedure has been performed by adding a small residual HS at long time.

are close to those obtained for other high-spin (HS) [Fe(sal$_2$-trien)]$^+$ compounds (see Table 1). At lower temperatures, the HS fraction remains constant and there is a ferromagnetic ordering with a T_c of 5.2 K, as usual for this type of compounds. In contrast to **1**, this compound does not present LIESST effect.

Discussion

The lifetime of the HS photoexcited state has been rationalized by Hauser,[27] on the basis of a non-adiabatic multiphonon relaxation model. In the framework of this theory, the metal–ligand distance is taken as the reaction coordinate, related to only one vibrational mode, namely the completely symmetrical one. This is the so-called SCC (single configurational coordinate) approach. Based on this theory, it is possible to estimate theoretically the rate constant for the HS → LS relaxation (k_{HL}) at different temperatures for the different ions that could exhibit the LIESST effect such as Fe^{II}, Fe^{III} or Co^{II}.[28] The main difference between these three ions is the bond length difference between the LS and the HS states, being typically 0.2 Å for Fe^{II}, 0.13–0.16 Å for Fe^{III} and 0.09–0.12 Å for Co^{II}. This change in bond length difference is expected to directly affect the decay of the photo-induced state, being much faster for Co^{II} than for Fe^{II} and Fe^{III}. Particularly, according to SCC theory, the low-temperature (tunneling regime) lifetime of the HS state for Fe^{III} spin-crossover compounds is expected to be of the order of milliseconds, whereas it can go from seconds to months for Fe^{II} spin-crossover compounds. According to such a short lifetime, it should be impossible to observe the decay of the photoinduced state for Fe^{III} by using standard SQUID techniques. However, as mentioned above, the LIESST effect has been observed by Sato in two Fe^{III} complexes, [Fe(pap)$_2$]$^+$ and [Fe(qsal)$_2$]$^+$.[18] This author attributed such an extraordinary result to the strong distortion of the Fe^{III} site from its octahedral geometry, which can be enhanced by the presence of strong intermolecular interactions, such as π–π stacking. Thus, when passing from the ideal octahedral site [Fe^{II}N$_6$] to a distorted [Fe^{III}N$_4$O$_2$] geometry, in addition to the completely symmetrical vibrational mode, other vibrational modes such as the bending mode should also be taken into account.[18,29] This results in a displacement between the potential walls of the HS and LS states, which is larger than that expected considering only the changes in metal–ligand distances, and could explain the long lifetime of the photogenerated HS state.

To evaluate the distortion of [Fe(sal$_2$-trien)]$^+$ in **1**, we have focused our attention on the differences between the 120 and 300 K structures of the compound as they are close to the LS and HS structures. The structure at 120 K corresponds to the LS structure since magnetic and Mössbauer data indicate that 100% of the Fe^{III} are in the LS state at this temperature. On the other hand, the structure at 300 K is close to the HS structure as magnetic data indicate that around 80% of Fe^{III} are in the HS state at this temperature.[14]

The first difference between the two structures is a shortening in the Fe–N and Fe–O bond lengths as expected for a spin-crossover. Thus, the average bond length differences are $\Delta r_{HL,Fe-N} = 0.149$ Å and $\Delta r_{HL,Fe-O} = 0.024$ Å. If we take into account that at 300 K about 20% of Fe^{III} remains in the LS state, we could expect $\Delta r_{HL,Fe-N} = 0.186$ Å and $\Delta r_{HL,Fe-O} = 0.03$ Å values between the LS and HS states of this compound. These values are very close to those exhibited by the two Fe^{III} compounds known to date presenting LIESST effect (in [Fe(pap)$_2$]X, $\Delta r_{HL,Fe-N} = 0.19$ Å and $\Delta r_{HL,Fe-O} = 0.05$ Å, and in [Fe(qsal)$_2$]Y, $\Delta r_{HL,Fe-N} = 0.18$ Å and $\Delta r_{HL,Fe-O} = 0.02$ Å).[18] Notice that these values are also similar to those reported for [Fe(sal$_2$-trien)][Ni(dmit)$_2$] ($\Delta r_{HL,Fe-N} = 0.188$ Å and $\Delta r_{HL,Fe-O} = 0.036$ Å)[30] which is the only other [Fe(sal$_2$-trien)]$^+$ salt reported so far for which both the LS and HS structural data are available.[31] This salt is the first example of [Fe(sal$_2$-trien)]$^+$ salt presenting a strong cooperative transition and wide hysteresis but no LIESST effect has been reported for this compound. Furthermore, the synthesis of this compound presents serious problems of reproducibility that could limit further studies.[32]

A second set of parameters accounting for angular and trigonal distortions from the ideal octahedron is provided by Σ and Θ parameters. However, Σ and Θ values of the 300 and 120 K structures lie in the range of those found for other HS and LS [Fe(sal$_2$-trien)]$^+$ compounds.[31] Therefore, it is difficult to get some conclusions from these parameters.

The third difference concerns the changes in selected bond angles (*cis* and *trans* N/O–Fe–N/O bond angles) between the LS and HS structures ($\Delta\measuredangle_{HL}$). In **1**, a value of $\Delta\measuredangle_{HL} = 93.64°$ is obtained. This value is intermediate between that of [Fe(pap)$_2$]$^+$ ($\Delta\measuredangle_{HL} = 136.06°$), for which LIESST effect is observed, and that of [Fe(acpa)$_2$]$^+$ (($\Delta\measuredangle_{HL} = 74.32°$), which does not present LIESST effect, but a larger value could be expected taking into account that there are still around 20% of Fe^{III} in the LS state in the structure solved at 300 K. Therefore, we can conclude that, in analogy with [Fe(pap)$_2$]$^+$, the strong distortion from the ideal octahedral geometry in **1** is at the origin of the LIESST effect.

In turn, a sharp structural difference between **1** and [Fe(pap)$_2$]$^+$ concerns the nature and dimensionality of the intermolecular interactions. Thus, while in [Fe(pap)$_2$]$^+$ the π–π 2D stacking between pyridine and phenyl rings seems to enhance the structural distortion of the LIESST complex, in **1**, π–π interactions between pairs of [Fe(sal$_2$-trien)]$^+$ complexes belonging to different chains coexist with edge-to-face CH–π and NH–π interactions. As a consequence, **1** shows a gradual spin-crossover with no hysteresis, while [Fe(pap)$_2$]$^+$ presents a cooperative spin-crossover with hysteresis. Furthermore, the decay of the photo-induced HS state of the two compounds follows a different relaxation kinetics. Whereas the time dependence of the HS fraction after photoexcitation of [Fe(pap)$_2$]$^+$ can be fitted to a sigmoidal-type curve as a result of self-acceleration of the HS → LS relaxation due to cooperative effects, the one from **1** can be fitted to a multiexponential curve with a fast component at earlier times and a long decay process at infinite times. The broad distribution of activation energies is the cause of this type of relaxation kinetics. These curves are typical of non-cooperative systems that rarely present a single-exponential behavior. It appears in poorly crystalline solids and in some cases it has been related to the presence of disorder in the structure in compounds presenting a cooperative spin-crossover.[33] Hence, it could have some relation with the disorder observed in the structure of **1** even it is only observed at high temperature. In any case, we can conclude that both the magnetic behavior and the decay of the photo-induced HS state in **1** indicate that in contrast to the

previous examples, cooperativity it is not a necessary condition to have LIESST effect in Fe^{III} compounds.

A second structural difference of **1** with respect to the other Fe^{III} compounds exhibiting LIESST effect is the presence of an anionic extended network (the bimetallic oxalate network) instead of a discrete small counterion. This rigid network could play a similar role in the stabilisation of the metastable HS state of **1** to that played by the strong π–π intermolecular interactions in $[Fe(pap)_2]^+$. In favour of this hypothesis are the numerous short contacts between the $[Fe(sal_2\text{-trien})]^+$ cations with the oxalate ligands, which are different in the low and high-temperature structures (see SI†). Maybe the interactions with the oxalate network enhance the distortion of the LIESST complex but, at the same time, they prevent a cooperative spin-crossover since they restrict the structural dimensionality to 2. Photomagnetic measurements on salts of $[Fe(sal_2\text{-trien})]^+$ and derivatives in different anionic environments are needed to clarify this point. This work is in progress in our group.[13d]

The question remains why no LIESST has been observed on the remaining 30% HS fraction at 10 K for compound **2**. Further work is necessary to answer to such question. For now, it remains unclear if the absence of LIESST is linked to: (a) a distortion effect and/or (b) the difference of rigidity between 2D and 3D networks and/or (c) the small amount of Fe^{III} that can be converted. As far as the distortion (a) is concerned, it would be helpful to compare the geometries of the $[Fe(sal_2\text{-trien})]^+$ complexes in the HS and the LS state. Unfortunately, this is not possible as the HS fraction remains at 70% at temperatures as low as 10 K. The influence of the rigidity of the network (b) can be seen in the fact that the contraction of the interlayer distance that follows the spin-crossover in **1** cannot be present in **2** that presents a more isotropic 3D network. Finally, the low amount of low spin fraction at low temperature (c) makes it difficult to observe the possible small increase of magnetic response under light, as it will be difficult to distinguish this increase from the important magnetic signal of the oxalate network. New compounds are to be synthesized, 2D and 3D, in order to have more data to draw conclusions.

Conclusions

In this work we have shown that the insertion of a $[Fe(sal_2\text{-trien})]^+$ complex cation into a 2D oxalate network results in a hybrid magnet with coexistence of magnetic ordering and photoinduced spin-crossover in compound **1**. The use of a molecular approach has led to the coexistence of two properties—ferromagnetism and photo-induced spin crossover—that normally do not appear together in the same compound. This could open the way to prepare switching magnets. Still, in the present case the photo-induced spin conversion of the inserted Fe^{III} complex has shown to have a negligible influence on the cooperative magnetic behaviour of the 2D oxalate network. This is not an unexpected result, as 2D oxalate networks with very different interlayer separations present similar T_c values. In this sense, hybrid compounds formed by insertion of these spin-crossover cations into a 3D oxalate network are expected to be more suitable, as this magnetic network has shown to be much more sensitive to the influence of an internal pressure. Unfortunately, the compound **2** obtained by insertion of a $[Fe(sal_2\text{-trien})]^+$ cation into a 3D oxalate network does not present LIESST effect.

Another remarkable result has been the observation of LIESST effect in **1**. This very rare and unexpected property in a Fe^{III} spin-crossover complex, has been attributed to the strong distortion exhibited by the metastable HS state. However, **1** has shown that, in contrast to what has been previously proposed, a cooperative spin-crossover is not a necessary condition to observe LIESST effect in Fe^{III} compounds. The presence of an extended anion network able to establish strong intermolecular interactions with the spin-crossover cation could also enhance this distortion. If this was true, the confinement of spin-crossover cations into extended networks could be a suitable strategy to induce LIESST effect on other Fe^{III} cations, or to improve LIESST properties in Fe^{II} complexes.

Finally, the discovery that $[Fe(sal_2\text{-trien})]^+$ complexes can present LIESST effect opens the way for the use of this compound in the preparation of new multifunctional switchable compounds with other properties different from the magnetic ones. An interesting possibility could be the switching of the conductivity in $[Fe(sal_2\text{-trien})]^+$ salts of $[Ni(dmit)_2]$ anions already reported in the literature.[34]

Acknowledgements

Financial support from the EU (SPINMOL ERC Advanced Grant to EC), the Spanish Ministerio de Ciencia e Innovación (Project Consolider-Ingenio in Molecular Nanoscience and projects MAT2007-61584 and CTQ-2008-06720) and the Generalitat Valenciana (Prometeo Program) are gratefully acknowledged.

Notes and references

1 (*a*) E. Coronado and P. Day, *Chem. Rev.*, 2004, **104**, 5419; (*b*) E. Coronado, C. Martí-Gastaldo, E. Navarro-Moratalla, A. Ribera, S. J. Blundell and P. J. Baker, *Nat. Chem.*, 2010, **2**, 1031.

2 (*a*) E. Coronado, M. C. Giménez-López, G. Levchenko, F. M. Romero, V. García-Baonza, A. Milner and M. Paz-Pasternak, *J. Am. Chem. Soc.*, 2005, **127**, 4580; (*b*) E. Coronado, M. C. Giménez-López, T. Korzeniak, G. Levchenko, F. M. Romero, A. Segura, V. García-Baonza, J. C. Cezar, F. M. F. De Groot, A. Milner and M. Paz-Pasternak, *J. Am. Chem. Soc.*, 2008, **130**, 15519.

3 M. Clemente-León, E. Coronado, C. Martí-Gastaldo and F. M. Romero, *Chem. Soc. Rev.*, 2011, **40**, 473.

4 (*a*) H. Tamaki, Z. J. Zhong, N. Matsumoto, S. Kida, M. Koikawa, N. Achiwa, Y. Hashimoto and H. Okawa, *J. Am. Chem. Soc.*, 1992, **114**, 6974; (*b*) H. Tamaki, M. Mitsumi, N. Nakamura, N. Matsumoto, S. Kida, H. Okawa and S. Ijima, *Chem. Lett.*, 1992, 1975; (*c*) C. Mathonière, S. G. Carling, D. Yuscheng and P. Day, *J. Chem. Soc., Chem. Commun.*, 1994, 1551; (*d*) C. Mathonière, J. Nutall, S. G. Carling and P. Day, *Inorg. Chem.*, 1996, **35**, 1201; (*e*) R. Pellaux, H. W. Schmalle, R. Huber, P. Fisher, T. Hauss, B. Ouladdiaf and S. Decurtins, *Inorg. Chem.*, 1997, **36**, 2301; (*f*) E. Coronado, J. R. Galán-Mascarós, C. J. Gómez-García, J. M. Martínez-Agudo, E. Martínez-Ferrero, J. C. Waerenborgh and M. Almeida, *J. Solid State Chem.*, 2001, **159**, 391; (*g*) K. S. Min, A. L. Rhinegold and J. S. Miller, *Inorg. Chem.*, 2005, **44**, 8433; (*h*) E. Coronado, J. R. Galán-Mascarós and C. Martí-Gastaldo, *J. Mater. Chem.*, 2006, **16**, 2685.

5 (*a*) S. Decurtins, H. W. Schmalle, P. Schneuwly and H. R. Oswald, *Inorg. Chem.*, 1993, **32**, 1888; (*b*) S. Decurtins, H. W. Schmalle, P. Schneuwly, J. Ensling and P. Gütlich, *J. Am. Chem. Soc.*, 1994, **116**, 9521; (*c*) M. Hernández-Molina, F. Lloret, C. Ruiz-Pérez and M. Julve, *Inorg. Chem.*, 1998, **37**, 4141; (*d*) E. Coronado, J. R. Galán-Mascarós, C. J. Gómez-García and J. M. Martínez-Agudo, *Inorg. Chem.*, 2001, **40**, 113; (*e*) F. Pointillart, C. Train, M. Gruselle, F. Villain, H. W. Schmalle, D. Talbot, P. Gredin, S. Decurtins and M. Verdaguer, *Chem. Mater.*, 2004, **16**, 832; (*f*)

M. Clemente-León, E. Coronado, C. J. Gómez-García and A. Soriano-Portillo, *Inorg. Chem.*, 2006, **45**, 5653.
6 (*a*) M. Clemente-León, J. R. Galán-Mascarós and C. J. Gómez-García, *Chem. Commun.*, 1997, 1727; (*b*) E. Coronado, J. R. Galán-Mascarós, C. J. Gómez-García and J. M. Martínez-Agudo, *Adv. Mater.*, 1999, **11**, 558; (*c*) E. Coronado, J. R. Galán-Mascarós, C. J. Gómez-García, J. Ensling and P. Gutlich, *Chem.–Eur. J.*, 2000, **6**, 552.
7 (*a*) S. Bénard, P. Yu, J. P. Audière, E. Rivière, R. Clèment, J. Ghilhem, L. Tchertanov and K. Nakatami, *J. Am. Chem. Soc.*, 2000, **122**, 9444; (*b*) S. M. Aldoshin, N. A. Sanina, V. I. Minkin, N. A. Voloshin, V. N. Ikorskii, V. I. Ovcharenko, V. A. Smirnov and N. K. Nagaeva, *J. Mol. Struct.*, 2007, **826**, 6.
8 (*a*) E. Coronado, J. R. Galán-Mascarós, C. J. Gómez-García and V. Laukhin, *Nature*, 2000, **408**, 447; (*b*) A. Alberola, E. Coronado, J. R. Galán-Mascarós, C. Giménez-Saiz and C. J. Gómez-García, *J. Am. Chem. Soc.*, 2003, **125**, 10774; (*c*) E. Coronado, J. R. Galán-Mascarós, C. J. Gómez-García, E. Martínez-Ferrero and S. Van Smaalen, *Inorg. Chem.*, 2004, **43**, 4808.
9 H. Okawa, A. Shigematsu, M. Sadakiyo, T. Miyagawa, K. Yoneda, M. Ohba and H. Kitagawa, *J. Am. Chem. Soc.*, 2009, **131**, 13516.
10 (*a*) R. Andrés, M. Gruselle, B. Malézieux, M. Verdaguer and J. Vaissermann, *Inorg. Chem.*, 1999, **38**, 4637; (*b*) R. Andrés, M. Brissard, M. Gruselle, C. Train, J. Vaissermann, B. Malézieux, J. P. Jamet and M. Verdaguer, *Inorg. Chem.*, 2001, **40**, 4633; (*c*) M. Clemente-León, E. Coronado, J. C. Dias, A. Soriano-Portillo and R. D. Willett, *Inorg. Chem.*, 2008, **47**, 6458.
11 J. R. Galán-Mascarós, E. Coronado, P. A. Goddard, J. Singleton, A. I. Coldea, J. D. Wallis, S. J. Coles and A. Alberola, *J. Am. Chem. Soc.*, 2010, **132**, 9271.
12 (*a*) C. Train, R. Gheorghe, V. Krstic, L. M. Chamoreau, N. S. Ovanesyan, G. L. J. A. Rikken, M. Gruselle and M. Verdaguer, *Nat. Mater.*, 2008, **17**, 729; (*b*) C. Train, T. Nuida, R. Gheorghe, M. Gruselle and S. Ohkoshi, *J. Am. Chem. Soc.*, 2009, **131**, 16838.
13 (*a*) R. Sieber, S. Decurtins, H. Stoeckli-Evans, C. Wilson, D. Yufit, J. A. K. Howard, S. C. Capelli and A. Hauser, *Chem.–Eur. J.*, 2000, **6**, 361; (*b*) E. Coronado, J. R. Galán-Mascarós, M. C. Giménez-López, M. Almeida and J. C. Waerenborgh, *Polyhedron*, 2007, **26**, 1838; (*c*) M. Clemente-León, E. Coronado, M. C. Giménez-López, A. Soriano-Portillo, J. C. Waerenborgh, F. S. Delgado and C. Ruiz-Pérez, *Inorg. Chem.*, 2008, **47**, 9111; (*d*) M. Clemente-León, E. Coronado and M. López-Jordà, *Dalton Trans.*, 2010, **39**, 4903.
14 M. Clemente-León, E. Coronado, M. López-Jordà, G. Mínguez Espallargas, A. Soriano-Portillo and J. C. Waerenborgh, *Chem.–Eur. J.*, 2010, **16**, 2207.
15 S. Decurtins, P. Gütlich, K. M. Hasselbach, A. Hauser and H. Spiering, *Inorg. Chem.*, 1985, **24**, 2174.
16 C. Enachescu, A. Hauser, J.-J. Girerd and M.-L. Boillot, *ChemPhysChem*, 2006, **7**, 1127.
17 (*a*) S. Hayami, Z.-Z. Gu, M. Shiro, Y. Einaga, A. Fujishima and O. Sato, *J. Am. Chem. Soc.*, 2000, **122**, 7126; (*b*) G. Juhász, S. Hayami, O. Sato and Y. Maeda, *Chem. Phys. Lett.*, 2002, **364**, 164.
18 S. Hayami, K. Hiki, T. Kawahara, Y. Maeda, D. Urakami, K. Inoue, M. Ohama, S. Kawata and O. Sato, *Chem.–Eur. J.*, 2009, **15**, 3497.
19 Crystal data for **1** at 300 K: $C_{27}H_{26}Cl_2CrFeMnN_4O_{14}$, $M = 864.21$, monoclinic, space group $P2_1/c$ (no. 14), $a = 12.096(5)$ Å;, $b = 32.135(5)$ Å;, $c = 9.467(5)$ Å;, $\beta = 111.981(5)°$, $V = 3412(2)$ Å^3, $Z = 4$, $\mu = 1.325$ mm^{-1}, $F(000) = 1748$, $T = 300(2)$K, 44282 reflections measured, 11352 unique ($R_{int} = 0.0589$), $R_1 = 0.0635$, w$R_2 = 0.1689$ for $I > 2\sigma(I)$. CCDC 807173. Crystal data for **1** at 250 K: $C_{27}H_{26}Cl_2CrFeMnN_4O_{14}$, $M = 864.21$, monoclinic, space group $P2_1/c$ (no. 14), $a = 11.9215(15)$ Å, $b = 31.910(3)$ Å, $c = 9.4841(11)$ Å, $\beta = 111.535(13)°$, $V = 3356.1(6)$ Å^3, $Z = 4$, $\mu = 1.348$ mm^{-1}, $F(000) = 1748$, $T = 250(2)$K, 43973 reflections measured, 11354 unique ($R_{int} = 0.0590$), $R_1 = 0.0530$, w$R_2 = 0.1240$ for $I > 2\sigma(I)$. CCDC 813345. Crystal data for **1** at 120 K: $C_{27}H_{26}Cl_2CrFeMnN_4O_{14}$, $M = 864.21$, monoclinic, space group $P2_1/c$ (no. 14), $a = 11.5561(3)$ Å, $b = 31.6369(7)$ Å, $c = 9.5457(3)$ Å, $\beta = 109.984(3)°$, $V = 3279.77(15)$ Å^3, $Z = 4$, $\mu = 1.379$ mm^{-1}, $F(000) = 1748$, $T = 120(2)$K, 26791 reflections measured, 10705 unique ($R_{int} = 0.0302$), $R_1 = 0.0477$, w$R_2 = 0.0951$ for $I > 2\sigma(I)$. CCDC 807172. Crystal data for **1** at 92 K: $C_{27}H_{26}Cl_2CrFeMnN_4O_{14}$, $M = 864.21$, monoclinic, space group $P2_1/c$ (no. 14), $a = 11.5602(4)$ Å;, $b = 31.6268(12)$ Å;, $c = 9.5237(4)$ Å;, $\beta = 110.199(4)°$, $V = 3267.8(2)$ Å^3, $Z = 4$, $\mu = 1.379$ mm^{-1}, $F(000) = 1748$, $T = 92(2)$K, 29715 reflections measured, 10846 unique ($R_{int} = 0.0557$), $R_1 = 0.0546$, w$R_2 = 0.1230$ for $I > 2\sigma(I)$. CCDC 813714. Crystal data of **1** at 180 K have been taken from ref. 14.
20 P. Guionneau, M. Marchivie, G. Bravic, J.-F. Létard and D. Chasseau, *Top. Curr. Chem.*, 2004, **234**, 97.
21 J. K. McCusker, A. L. Rheingold and D. N. Hendrickson, *Inorg. Chem.*, 1996, **35**, 2100.
22 M. Marchivie, P. Guionneau, J.-F. Létard and D. Chasseau, *Acta Crystallogr., Sect. B: Struct. Sci.*, 2005, **61**, 25.
23 C. Janiak, *J. Chem. Soc., Dalton Trans.*, 2000, 3885.
24 L. Néel, *Ann. Phys.*, 1948, **3**, 137.
25 J.-F. Létard, *J. Mater. Chem.*, 2006, **16**, 2550.
26 A. Hauser, J. Adler and P. Gütlich, *Chem. Phys. Lett.*, 1988, **152**, 468.
27 A. Hauser, *J. Chem. Phys.*, 1991, **94**, 2741.
28 A. Hauser, *Top. Curr. Chem.*, 2004, **234**, 155.
29 S. Schenker, A. Hauser and R. M. Dyson, *Inorg. Chem.*, 1996, **35**, 4676.
30 S. Dorbes, L. Valade, J. A. Real and C. Faulmann, *Chem. Commun.*, 2005, 69.
31 R. Pritchard, S. A. Barrett, C. A. Kilner and M. A. Halcrow, *Dalton Trans.*, 2008, 3159.
32 C. Faulmann, P. A. Szilágyi, K. Jacob, J. Chahine and L. Valade, *New J. Chem.*, 2009, **33**, 1268.
33 V. Mishra, R. Mukherjee, J. Linares, C. Balde, C. Desplanches, J.-F. Létard, E. Collet, L. Toupet, M. Castro and F. Varret, *Inorg. Chem.*, 2008, **47**, 7577.
34 C. Faulmann, S. Dorbes, J. A. Real and L. Valade, *J. Low Temp. Phys.*, 2006, **142**, 261.